



HAL
open science

A New Structural Study for an Old Quasicrystal

M. Laridjani

► **To cite this version:**

M. Laridjani. A New Structural Study for an Old Quasicrystal. Journal de Physique I, 1996, 6 (10), pp.1347-1364. 10.1051/jp1:1996140 . jpa-00247249

HAL Id: jpa-00247249

<https://hal.science/jpa-00247249>

Submitted on 4 Feb 2008

HAL is a multi-disciplinary open access archive for the deposit and dissemination of scientific research documents, whether they are published or not. The documents may come from teaching and research institutions in France or abroad, or from public or private research centers.

L'archive ouverte pluridisciplinaire **HAL**, est destinée au dépôt et à la diffusion de documents scientifiques de niveau recherche, publiés ou non, émanant des établissements d'enseignement et de recherche français ou étrangers, des laboratoires publics ou privés.

A New Structural Study for an Old Quasicrystal

M. Laridjani

Laboratoire de Physique des Solides (*), Université Paris-Sud, 91405 Orsay Cedex, France

(Received 10 January 1996, revised 19 April 1996, accepted 27 June 1996)

PACS.61.44.Br – Quasicrystals

Abstract. — In this paper, we have described the experimental evidence for the polyhedral order in metastable Al-Mn alloy (icosahedral phase). We have used the anomalous diffractometry technique to identify the X-ray patterns of this alloy. For the first time, the radial distribution function of the diffuse rings scattered by this alloy is obtained by applying this new technique. Unlike previous methods used for interpreting the X-ray patterns of this phase, we have introduced a new method of separation for interpreting X-ray patterns. The X-ray diffraction pattern has been numerically resolved into a broad diffuse halo and sharp lines. Using this procedure the correlation position was deduced from a high quality interference function. We have not been able to explain either the origin of the sharp lines or the relationship of the two parts responsible for the lines and rings. In order to explain the above we need an appropriate geometrical model and some structural information on the medium range order of the atoms causing scattered rings. This information is contained in the partial pair-pair correlation function of the coherent background. The result of this work may be of aid in order to comprehend the “genetic” relationship between the structure of the crystalline, amorphous FK phases and this new metastable alloy or icosahedral phase.

1. Introduction

Many attempts have been made to explain the atomic arrangements of a new metastable intermetallic phase (Al-Mn) which has been obtained by the melt spinning technique. The icosahedral point group symmetry ($\bar{3} \bar{5} m$) of the electron diffraction pattern of this phase is inconsistent with translational of periodicity.

Various non-crystalline mathematical models have been proposed for the above structure, namely the quasi crystalline model. These models can be classified into two categories:

- 1) The first one is based on a Penrose aperiodic lattice which can be constructed by the projection of a six-dimensional space (Levine *et al.* [1])
- 2) The other is a random connection of icosahedra (RCI-Shechtman *et al.* [2]). All these models predict sharp diffraction lines despite their aperiodic nature.

Other investigators have proposed a crystal structure with a unit cell to explain the X-ray diagram of this phase [3–5].

(*) Associé au CNRS (URA D 0002)

Although these models account for the symmetry or the pseudosymmetry, the exact atomic arrangement in this alloy is still controversial and has not been confirmed experimentally. This is due to two facts:

- a) These alloys have been obtained only by splat cooling technique, in which the sample is always in the form of a polycrystal. The structural determination by the powder method is not an easy task. It can be known precisely if the structural studies are performed with single crystals.
- b) It is well-known that the metastable alloys obtained by melt spinning are not homogeneous samples. The non-homogeneity of the sample is related to the different rates of cooling, in cooling of the molten alloy on a rotating metal wheel or another substrate [6,7].

In addition, despite the prediction of obtaining an X-ray pattern with discrete lines, a precise diffraction diagram indicates intrinsic diffused scattered rings [8,9]. Whereas in *classical diffractometry* the diffuse coherent rings cannot be distinguished from the non-coherent scattering, the total background (the diffuse coherent rings + non-coherent scattering) is ignored and excluded from the total diffracted intensity. However, X-ray diagrams have been obtained carefully by using new techniques of Anomalous Diffraction (A.D.). X-ray diagrams of this alloy taken using this technique consist of sharp lines superimposed on the diffuse rings [10,11].

The purpose of this work is the structural study of Al-Mn, obtained by melt spinning techniques, *without the exclusion* of the diffused scattering part of the diffracted intensity. This new technique of anomalous diffractometry has been used to identify the X-ray pattern of this new metastable phase.

2. Experimental Method

Alloys were prepared with rapid quenching from the melt on the surface of a single Cu roller. With the help of this technique, samples of 0.5 mm thickness with lateral dimensions of 70 mm × 8 mm were obtained for this experiment.

The availability of synchrotron radiation and the rotating target permit an easy wavelength selection. Thus patterns with a chosen wavelength, either far from or near the absorption edge of an atom can be obtained. The dependence of the atomic scattering factor, f , of an element on the energy of the incident X-ray beam is sufficient for changing the contrast between the different components of a material.

A new diffractometer has been designed for this purpose. For separating fluorescence and incoherent radiation from the coherent component, the scattered beam is recorded by an energy dispersive detector of lithium-drifted silicon. The detector is connected to a preamplifier and a pulse processor. The pulse processor is a sophisticated signal processing unit which provides a linear amplification, noise filtering, pulse pile-up rejections and a life-time correction. The solid state detector has an energy resolution of 150 eV at 8 keV. Its resolution in energy does not only permit the elimination of fluorescent radiation from the sample but it also partially removes the incoherent Compton scattering.

The very simple geometrical construction of the goniometer (in contrast with the ideal X-ray goniometer) is due to the parallel beam and the X-ray optical arrangement.

The diffractometer can be optimised to reduce the deviation of the observed diffraction profile lines from the ideal profile (Delta Function). This technique facilitated the important background and Compton corrections, enhancing the quality of X-ray patterns and achieving high resolution. Thus recordings of low intensities and high Bragg reflections with numerous wavelengths in the same experiment can be performed.

All these advantages have allowed the creation of a new technique called Anomalous Diffraction (AD). This technique was used intensively to obtain partial distribution functions for the structural study of metallic amorphous alloys. The details of the A.D. method can be found elsewhere [12].

The diffracted intensity was measured in transmission and reflection at the following energies:

Below and at Mn and Zr, K absorption edges for the Al-Mn alloy ($E = 6529, 6500, 6339, 17984$ eV) and below and at the Cu and Zr, K absorption edges for a "control" sample of the Cu ($E = 8980$ eV).

Figure 1 shows X-ray patterns of pure polycrystalline Cu, in the form of a powder, obtained by the A.D. technique. The wavelength was selected to be 0.6922 \AA , about 1 eV further from the K absorption edge of Zr element (17984 eV) and far from the K edge of Cu. Figure 1b shows only discrete Bragg reflections without any background. But if the selected wavelength, $\lambda = 1.3806 \text{ \AA}$, is around 6 eV of the CuK absorption edge ($E = 8980$ eV) then the Bragg reflection of Cu will be superimposed on the background.

It is well-known that this background is mainly due to a secondary fluorescent radiation which causes a high incoherent background (Fig. 1a). The presence of this background, is due to the resolution of the detector. The resolution of the solid state detector near the K edge of Cu is sufficient to resolve the fluorescent line of K_α from K_β but not adequate enough to resolve K_β from coherent diffracted beams from the sample. Therefore, an accurate estimation of K_β is necessary so that it can be subtracted from the diffracted intensity of the photon scattered elastically from the sample.

Due to predictions in theoretical works, we have assumed a K_β/K_α ratio which is independent of the excitation energy. A precise measurement of the two fluorescence lines gives $K_{\beta_{Cu}}/K_{\alpha_{Cu}}$ a value of 0.17 eV instead of 0.19 given in reference [13]. The diffracted intensity is normalized to this value. The result is Figure 1c which shows the absence of background and only the presence of the Bragg reflections.

Hence, by this procedure of normalization a powder pattern of a polycrystalline sample can be obtained. This pattern consists of discrete Bragg reflections, with symmetrical lines and a resolution of about $\text{FWHM} = 9 \times 10^{-3}$ ($K = 1.43 \times 10^{-3} \text{ \AA}^{-1}$).

3. Results and Discussion

Figure 2 shows X-ray patterns of a rapid quenched Al 25 wt% Mn obtained with a photon energy of 17984 eV near the K edge of Zr ($\lambda = 0.6922 \text{ \AA}$) and near the MnK edges ($E = 6529$ eV, 8 eV below the Mn edge). After normalization (see [12]), these diagrams still consist of sharp lines superimposed on the diffused rings. Therefore the background is *intrinsic* to the sample. To interpret such an X-ray diagram consisting of a mixture of sharp lines and diffused rings, it would be convenient to separate the lines from the coherent background (rings).

Here, a new procedure is proposed in which the diffraction pattern has been numerically resolved into rings and sharp lines by a computer program with respect to the following three hypotheses:

- a) The law of conservation of coherent intensity scattered by the sample. Meaning that the intensity (I) of each point on the X-ray diagram is the sum of the intensities scattered by two parts; the sharp lines, part (I_1) and the background, part (I_2) in the sample. Then:

$$I_{\text{total}} = I_1 + I_2$$

- b) The intensity of each point of the background curve should be:

$$I_2 \leq I_{\text{total}}$$

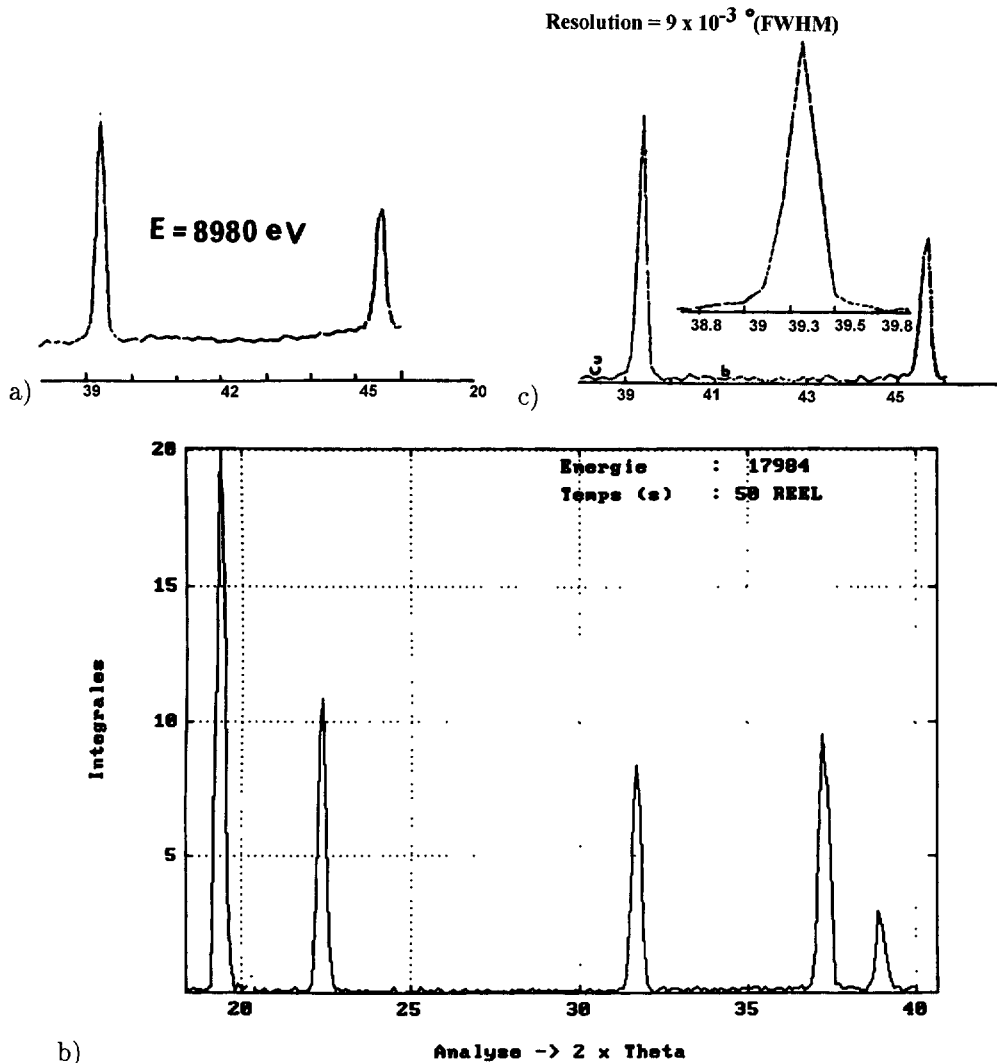


Fig. 1. — X-ray diagram of polycrystal of Cu (control sample) with a selected λ ($E = 8980$ eV) near K absorption edge of Cu ($\lambda = 1.38059$ Å): a) with non-coherent B.G., b) without B.G., far from the K edge of the Cu, c) after normalization without non-coherent B.G.

c) The intensity of any point of the X-ray diagram where there is no line should be:

$$I_1 = 0 \quad I_2 = I_{\text{total}}$$

By using these hypotheses, the lineless sections will be conserved as a part of the background curve. By linear interpolation the missing part of the background curve and the sharp line diagrams will be constructed in order to obtain the coherent background (rings) X-ray diagram and the sharp line spectrum (see Fig. 3c). This procedure produces two diagrams: a sharp line spectrum and rings.

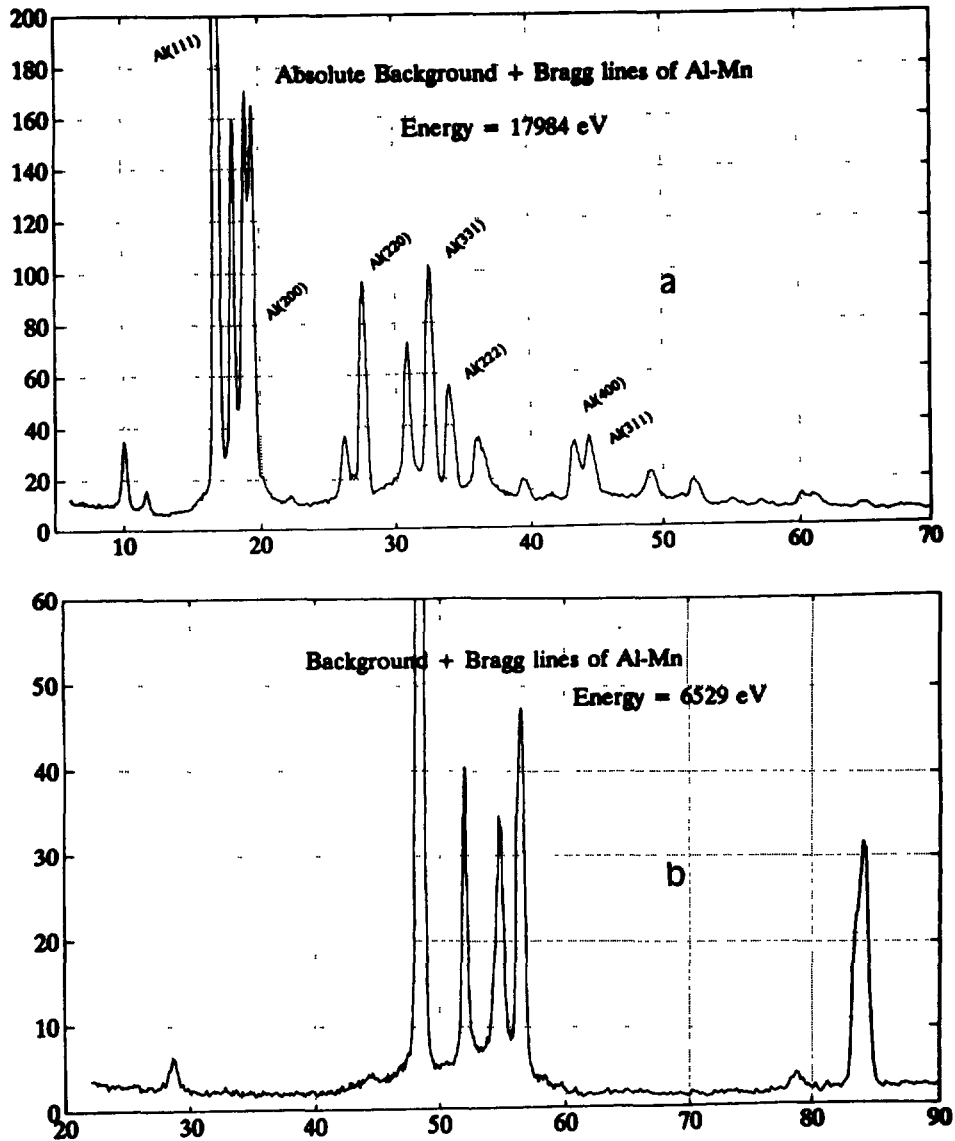


Fig. 2. — The X-ray pattern of a metastable Al-Mn. This diagram consists of sharp lines superimposed on the rings (coherent B.G.). Figures a, b show mixed X-ray patterns of Al-Mn with the energy near and far from the K absorption edge of Mn. a) Near the Zr K-edge, $E = 17984$ eV, $\lambda = 0.6822$ Å. b) Near the Mn K-edge, $E = 6529$ eV, 8 eV below of Mn edge.

3.1. SPECTRUM OF SHARP LINES. — Figure 4a indicates a spectrum of sharp reflections. The feature of this diagram is similar to the one reported by Bancel *et al.* [14]. They indexed the reflection lines of this high resolution X-ray diagram obtained by synchrotron radiation in

three different phases:

- the orthorhombic equilibrium Al_6Mn (2-3%);
- the fcc Al;
- a third phase which they called the icosahedral phase.

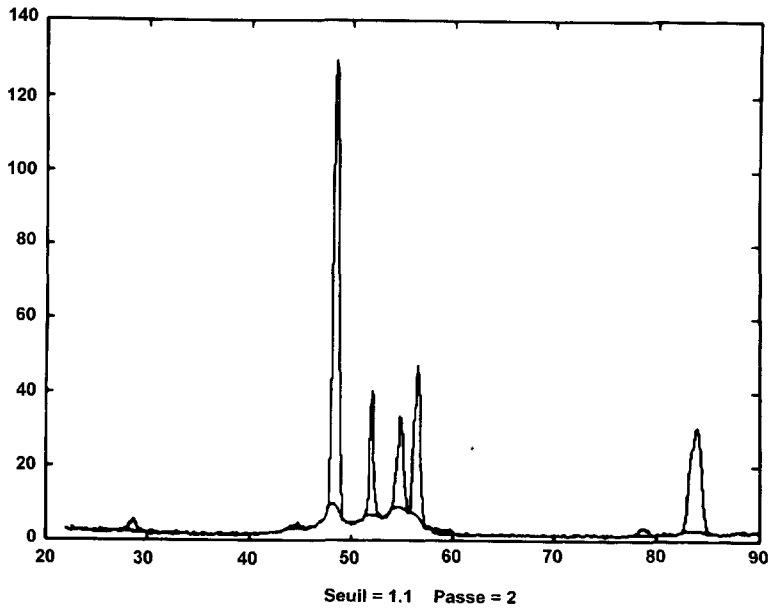
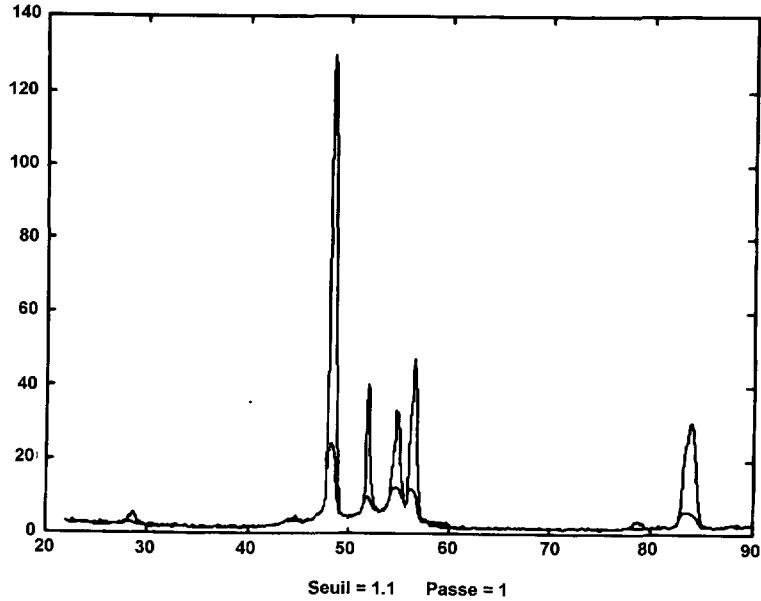


Fig. 3. — These figures show different stages of separation of Figure 2b. These mixture X-ray patterns can be numerically resolved by special procedures into two diagrams: ring diagrams, line diagrams.

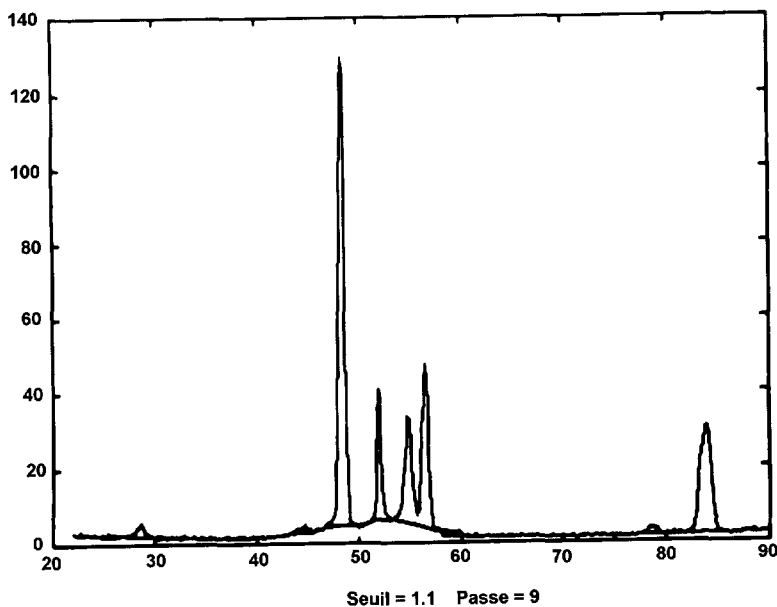


Fig. 3. — (Continued.)

The corresponding “ d ” spacings and their respective intensities are given in Table I and they are compared to the results of other investigators.

This phase was indexed by the proposed model of Levine and Steinnardt. At their maximum position *only* 13 reflections of the X-ray pattern match with 30 calculated reflections of the model.

Previous to this paper, Schechtman and Blech [15] reported an X-ray diagram obtained by classical diffractometry, using $\text{CuK}\alpha$, of a new metastable phase of Al-Mn. Three compositions of this alloy (18, 22 and 25.3 Mn wt%) have been quenched. A non crystalline structural model with an assembly of icosahedral units, joined by their edges to each other, has been reported by them. They claim to have *quite a good agreement* of the calculated spacings (d) with those obtained experimentally. Nine reflections have been measured of which three reflections (3.83, 2.056 and 1.497 Å) have not been identified. The relative intensity I of these reflections corresponds respectively to 7, 75 and 7 cannot be considered as weak reflections [15].

Seven days later they and two more investigators submitted a new paper to report the same metastable phase of Al-Mn which crystallizes in a non-crystallographic symmetry of $(\bar{3} \ 5 \ m)$. They claimed that their X-ray pattern could not have been indexed by any Bravais lattice. They then suggested a long range orientational order without reporting the “ d ” spacings and the observed relative intensity of each reflection line [16]

A year later, Pauling proposed a large cubic cell ($a = 26.7 \text{ \AA}$) for indexing the spacings measured from the classical X-ray pattern ($\lambda = \text{CuK}\alpha$) of this new metastable phase which was obtained by Schechtman and Blech [15] (see Tab. I). From this unit cell, 22 “ d ” spacings were predicted with which only ten interplanar spacings present on the X-ray pattern are comparable. In the structural interpretation, the absence of (111), (311) (333) and (511) reflections in the X-ray powder diffraction pattern has been explained, (see Refs. [3,4]).

Later on in 1988 other investigators [5] proposed a large tetragonal unit cell as the crystal structure of this new phase. For this structural analysis the interplanar spacing of Bancel *et*

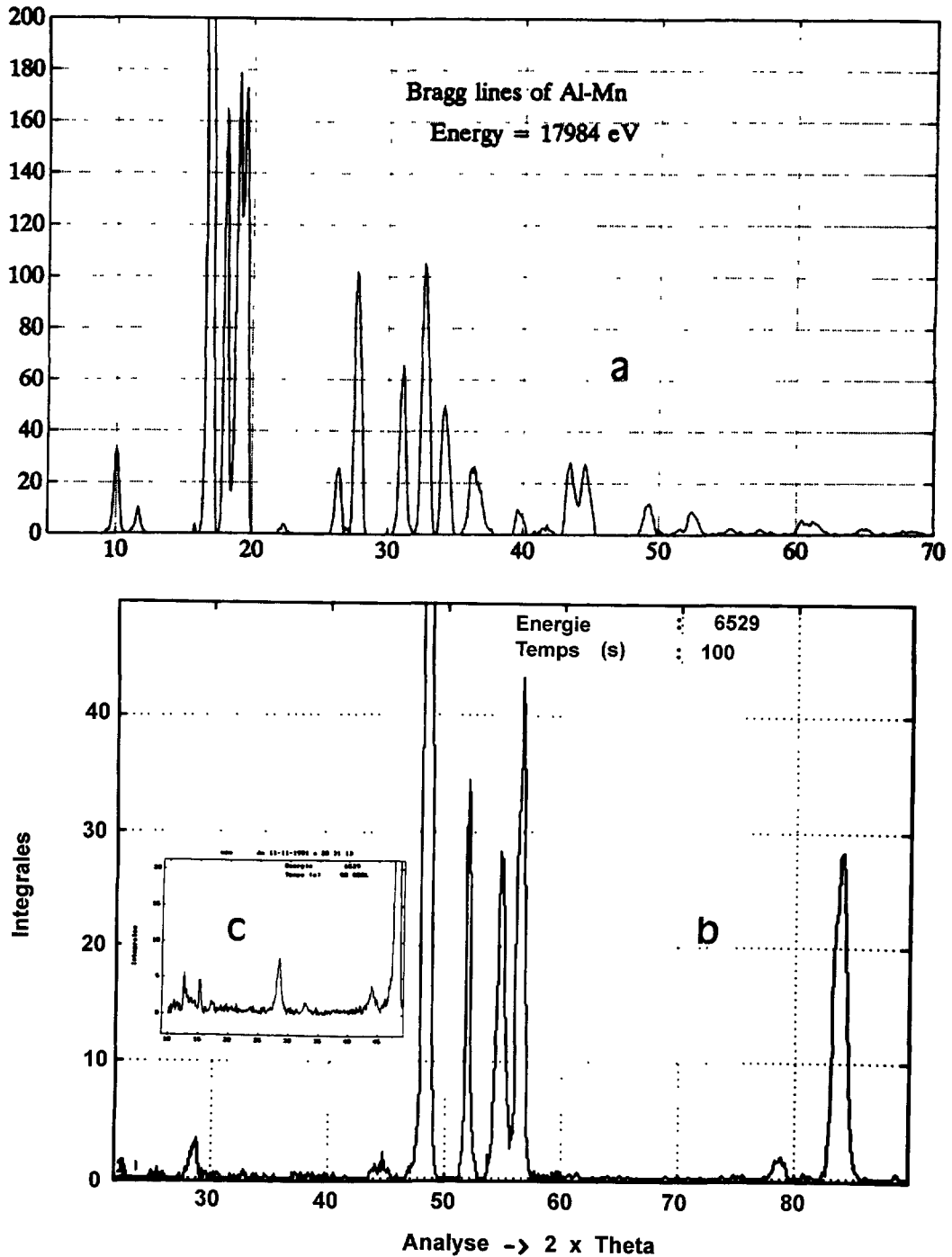


Fig. 4. — a) The line spectrum of metastable Al-Mn alloy $\lambda = \lambda_1 = 0.689 \text{ \AA}$, $E = E_1 = 17984 \text{ eV}$ (far from K absorption edge of Mn). b) Line spectrum of metastable Al-Mn alloy (near to the Mn edge) $\lambda = \lambda_2 = 1.8988 \text{ \AA}$, $E = E_2 = 6529 \text{ eV}$ ($E = 6539 \text{ eV}$ -K edge of Mn). c) Zoom of $2\theta = 10^\circ - 48^\circ$ for this wavelength.

Table I. — Observed interplanar spacing (\AA) and observed relative intensities from the metastable Al_6Mn phase.

			This work		
$\lambda = 1.54 \text{ \AA}$ Schechtman	$\lambda = 1.54 \text{ \AA}$ Pauling	$E = 14600 \text{ eV}$ Bancel	$E = 1798 \text{ eV}$ $\lambda = 0.6822 \text{ \AA}$	$E = 6529 \text{ eV}$ $\lambda = 1.89885 \text{ \AA}$	$E = 2 \times 6529 \text{ eV}$ $\lambda = 0.9494 \text{ \AA}$

●

d	I	d	I	d	I	d	I	d	I	d	I
3.3830	7	3.8500	7	3.850	22	3.9100	20	3.87	15	3.895	25
3.3330	2	3.3400	2	3.356	8	3.3750	9	3.35	< 1	3.389	6
						2.5100	1			3.700	6
2.1681	100	2.1680	100	2.170	100	2.1800	94	2.169	100	2.184	86
2.0624	75	2.0600	150	2.065	78	2.0660	100	2.06	85	2.100	100
2.0560	75	-	-	-	-	-	-	-	-	-	-
						1.7639	7				
1.4970	7	1.4946	7	1.496	11	1.4937	21.5	1.495	9	1.50	18
						1.4600	2				
1.2760	21	1.2765	21	1.275	20	1.2723	42			1.2782	40
1.1000	6	1.0994	6	1.110	6	1.0920	14				
1.0860	5	1.0856	5	1.090	7	1.0120	6				

● Before the first reflection reported by Bancel ($d = 3.85 \text{ \AA}$) there are at least 17 reflections (+)

d	I	d	I
10.78	0.7	6.390	< 0.5
9.470	0.6	6.2410	< 0.5
8.720	1.2	6.1360	< 0.5
8.190	< 0.5	5.840	1.1
7.900	< 0.5	5.410	< 0.5
7.500	< 0.5	5.100	< 0.5
7.178	< 0.5	4.142	< 0.5
6.790	< 0.5	4.067	< 0.5
6.169	< 0.5		

(+) This is the reason of our analogy with Al-Ge system.

al. [14] was used (see Tab. I). Table I shows that there are remarkable discrepancies between the “ d ” values and the intensities.

Even for equilibrium alloys, the absence of the first reflection is a most serious handicap for any attempt at structural analysis. Indeed it is well-known that the indexability of a powder pattern is related to the accuracy in resolving the powder reflection or the peak to background ratio. In any case their combined effect is devastating for determining the indexability of a pattern.

Another problem in identifying metastable phases in splat-quenched alloys is the separation of the X-ray reflection due to the various phases. It becomes especially problematic where phases co-exist with the intermetallic equilibrium phase over this composition range as in the Al-Mn system. Al-Ge would be an ideal system for demonstrating this problem. Contrary to the Al-Mn system, in the Al-Ge system there are no intermediate phases (*cf.* Ref. [7]). Due to the complexity of the X-ray diffraction pattern of these metastable phases the total number of reflections observed by various investigators were not similar. Consequently different unit cells (cubic, hcp, 4 different tetrahedrals, rhombohedral and monoclinic) were assigned. These discrepancies in the X-ray powder pattern could be either due to the lack of control over the cooling rate, or a weak separation of the lines of different phases, or not grouping well the diffraction lines. In the case of Al-Mn, the presence of at least four intermediate phases in the equilibrium diagram of this region make the interpretation of the X-ray pattern of each phase more difficult.

Figure 4 shows sharp reflection diagrams obtained at $E = 6529$ eV and $E = 17984$ eV where the position and intensity of each reflection can be measured precisely (Tab. I). The position of all reflections at $E = 6529$ eV *remains untouched* compared to the d spacings derived from the radiation at $E = 17984$ eV. Obviously, the intensity of the reflections changes considerably for $E = 6529$ eV (-8 eV below MnK absorption edge). For instance at $d = 3.35$ Å the reflection vanishes and the height of the other reflections change. *i.e.*, the intensity of the reflection at $d = 3.87$ Å changes to 15 instead of 20 and the reflection of $d = 2.169$ Å becomes the strongest line of this diagram (*cf.* Tab. I).

As we have mentioned the variation of the relative intensity is due to the rapid changes of the scattering factor (f) as a function of the photon energy near the absorption edge of one atomic species. In this system Mn is mainly responsible for this reflection. *It is worth mentioning that this dispersion effect is not an artifact.* This is due to the fact that, in the same experiment, the performance of anomalous diffractometry would allow the possibility of selecting the harmonic ($2E$) of the previous radiation E , which is close to the Mn absorption edge. Figure 5 shows the X-ray diagram derived from the $2E$ radiation which is far from the Mn edge. The effect of anomalous dispersion is the disappearance of the reflection of $d = 3.35$ Å and the appearance of a change in the relative intensity of the other reflection which matches with the sharp line diagrams derived from $E = 17984$ eV. Note that this phenomenon permits the separation of mixture patterns which belong to different metastable intermediate phases. Therefore the spectrum of lines can be compared significantly by measuring, from different wavelengths, the relative intensity, the maximum position, and the profile of each line.

Here the relative intensity can be defined as the ratio of the integrated intensity of each line to the integrated intensity of the strongest line. Hence a related structure factor $F(hkl)$ of each line can be obtained accurately in contrast to those before the separation procedure.

On the other hand in this method scattered radiation for very small Bragg angles from the sample is not over shadowed by a direct beam. Before the first reflection reported by Bancel *et al.* ($d = 3.85$ Å), we are able to measure at least 17 reflections (*cf.* Tab. I). As mentioned before, these weak reflections are indispensable for the structural determination of the metastable phase (*cf.* Tab. I). The high resolution of this technique permits us to identify

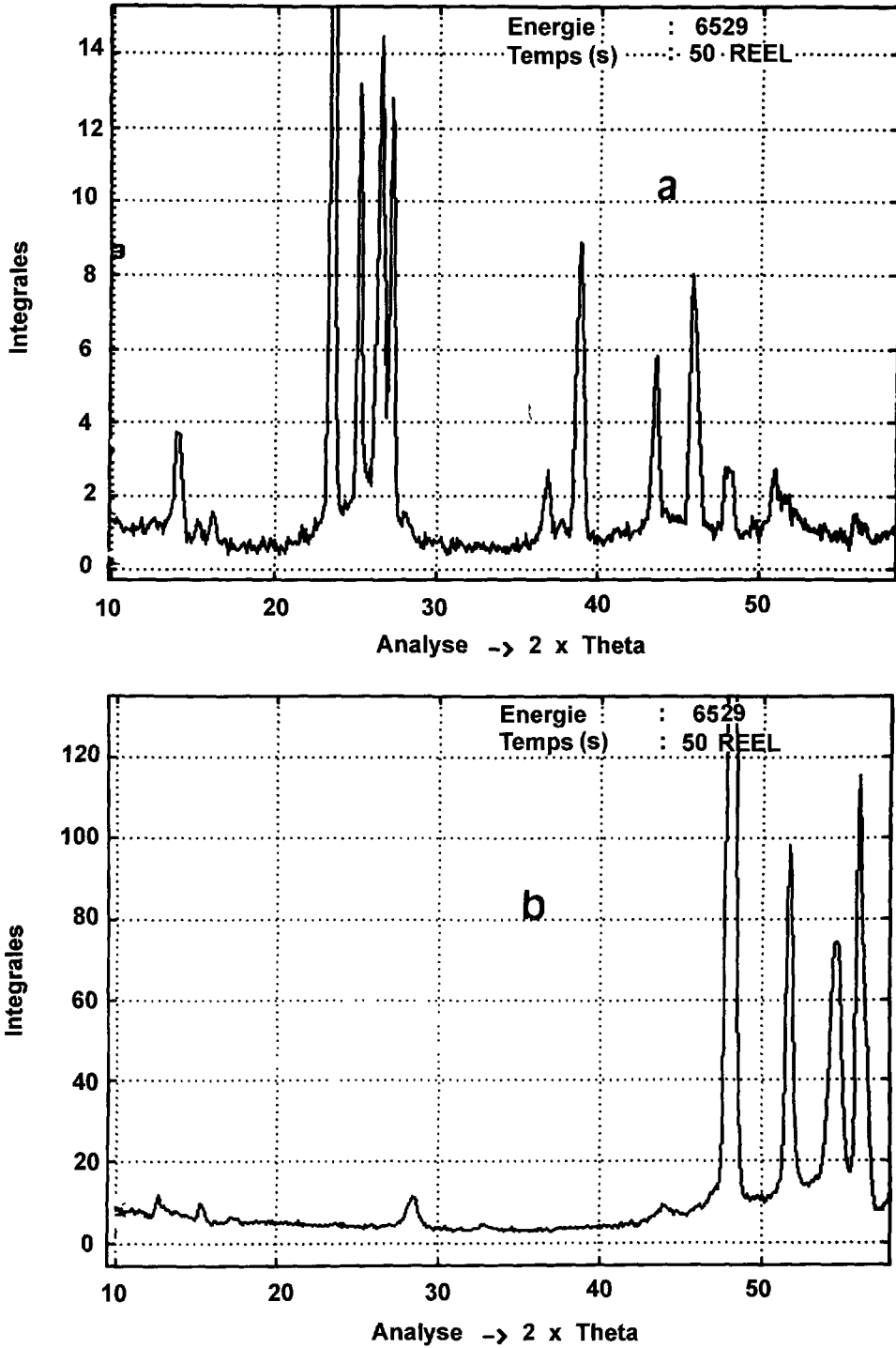


Fig. 5. — X-ray pattern of Al-Mn obtained in the same experiment as Figure 4b. a) $\lambda = \lambda_3 = \lambda_2/2 = 0.9494 \text{ \AA}$, b) $E = E_2 = 6529 \text{ eV}$.

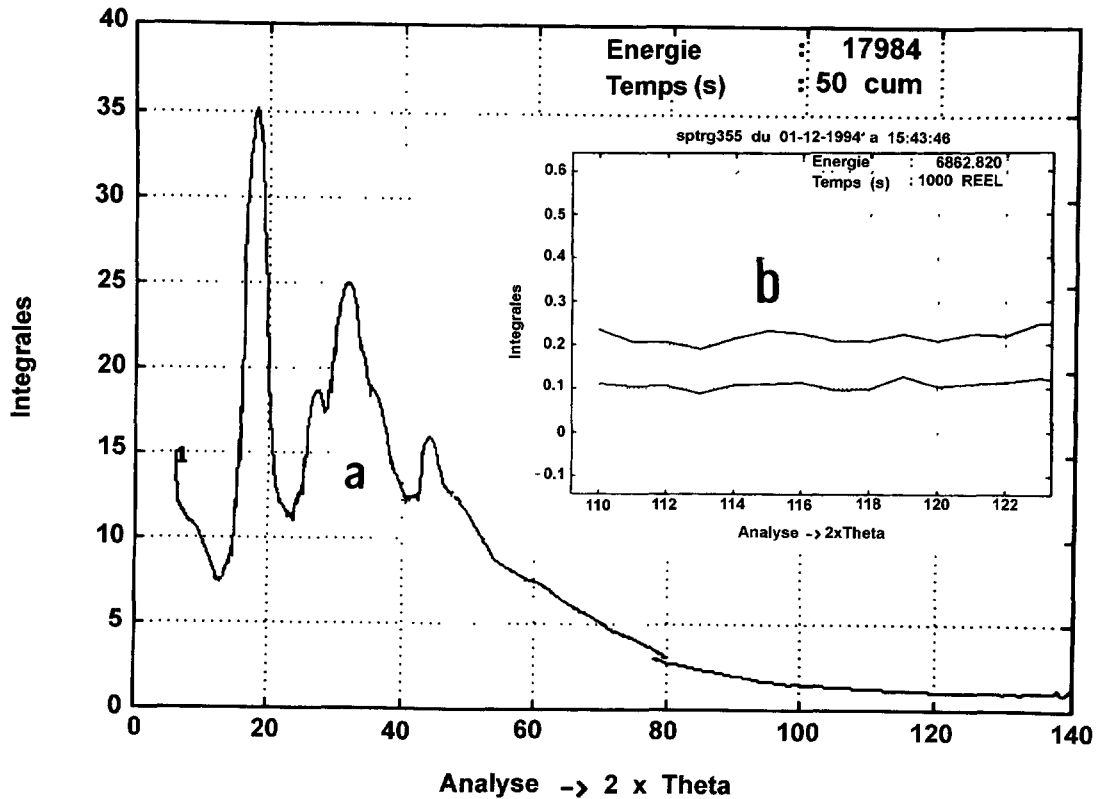


Fig. 6. — a) The spectrum of rings or the coherent diffracted intensity $I_d(\theta)$ (Fig. 5). b) This Figure shows the reliability of this technique for two different experiments.

all Al reflections up to $2\theta = 140^\circ$ ($K = 18 \text{ \AA}^{-1}$) and separate them from coherent scattered beams for the new phase.

The lattice parameter of a dilute solid solution was measured to be $a = 4.046 \text{ \AA}$ instead of 4.049 \AA which is the value of the lattice parameter of pure Al reported in literature. From this we can conclude that according to the analogy made with two systems (Al-Mn and Al-Ge), *the missing first reflection*, modeling in the non-crystalline structure or the proposed unit cell is only a belief arising from a short cut which especially excludes the coherent background scattered from the quenched Al-Mn sample.

3.2. "RINGS" DIAGRAM. — Figure 6 shows a spectrum of rings, after the separation of the lines from the mixed diagram (Fig. 3c). This diagram indicates the diffracted intensity $I_c(2\theta)$ scattered from the "non-crystalline" part of this alloy.

It is obvious this separation can be performed if the *ideal* powder diffractometry is used. For an ideal powder diffractometry, a random orientation of the grains in the sample, a strict monochromatic beam and an ideal X-ray optics are recommended. This type of performance in classical X-ray diffractometry would be a difficult task. Our technique facilitates the achievement of an important background and Compton corrections for obtaining a high quality X-ray pattern with a high resolution and without any statistical noise. Figure 6b shows the reliability of this technique in the case of a disordered material at a high K . ($K = \frac{4\pi \sin \theta}{\lambda}$). Due to this

performance, we believe that this procedure of separation is justified.

The first halo of this diffracted intensity $I_c(2\theta)$ indicates the presence of a short range correlation and the absence of a long range order. Hereafter an essential question can be brought up: what is the relationship between the part responsible for the fine lines and the ring diagram ?

In order to answer this question we would have to use the "amorphography" technique and such a technique would require a high quality interference function.

3.2.1. Interference Function. — To acquire the interference function, $J(K) = \frac{I_c(K)}{Nf^2(K)}$, the intensity was obtained from rings diagram which can be considered as a scattering of an isotropic part of the sample. Here N is the total number of the diffracting atoms of form factor and K is the scattering vector. After absorption corrections the interference functions were derived from the data using the classical procedure of normalization: dividing the experimental intensity by a calculated gaseous scattering intensity adjusted to large value of K . Small errors in this normalization are detected and corrected by taking into account the low R (\AA) contribution to the radial distribution function:

$$W(r) = r(P(r) - 1) = (2\pi^2\rho_0)^{-1} \int_0^\infty F(K) \sin Kr dr \quad ,$$

obtained by the Fourier transform. In other words, the experimental $I_c(K)$ was analytically corrected. According to this argument, there are no interatomic distances smaller than the nearest neighbourhood distances. This indicates that the curve below the first peak of the R.D.F. has a slope of " -1" (*i.e.* below this peak there is a probability $P(r) = 0$ of finding an atom at a distance r from a reference atom).

Figure 7 displays the reduced interference function, ($F(K) = K[J(k) - 1]$), of an isotropic part of a metastable Al-Mn alloy.

The general feature of this curve looks similar to the theoretical interference function of Dense Random Packing (DRP) of a non-equal sized hard sphere model [17]. In this figure, the first peak appears at $K_1 = 2.95 \text{ \AA}^{-1}$ and the second peak appears at 4.90 \AA^{-1} with a typical shoulder at the high K side obtained from the DRP model, and this interference function lead us to believe that the DRP model is a good approach for describing the local order of this curve. The reasons for this assumption are: the maximum position of the peaks, the existence of the shoulder at $K_3 = 5.9 \text{ \AA}^{-1}$, the ratio of the first peak position compared to the second peak position (*i.e.* $K_2/K_1 = 1.66$) which is the signature of the (DRP) model.

This model was proposed earlier for the metal-metalloid amorphous alloys in which the local order has an icosahedral symmetry (five fold symmetry). Therefore it can be suggested that the structure of the part responsible for these rings is based on the icosahedral packing of 12 atoms around the central atom (coordination number CN = 12).

This cluster was referred to Hume-Rothery [18] as a Frank unit in a supercooled liquid. They join together to constitute a pentagonal chain in the liquid to provide a nuclei for the growth of Frank-Kasper (FK) crystalline phase. It has been shown that it is possible to congeal this kind of liquid to form a glassy FK phase [12, 19]. From the interference function which has been obtained from the coherent backgroundings, we can conclude that the memory of the Frank chain in the liquid remains in the part that scatters the coherent background. This local configuration (icosahedron) cannot tile perfectly in a 3 D euclidean space where all the atoms are icosahedrally (CN = 12) coordinated. Frank and Kasper argued that the polyhedral cages of complex alloys of transition metals with icosahedral packing and polyhedral cages of CN = 14, CN = 15, and CN = 16 atom coordination will tile up in normal space. It has been

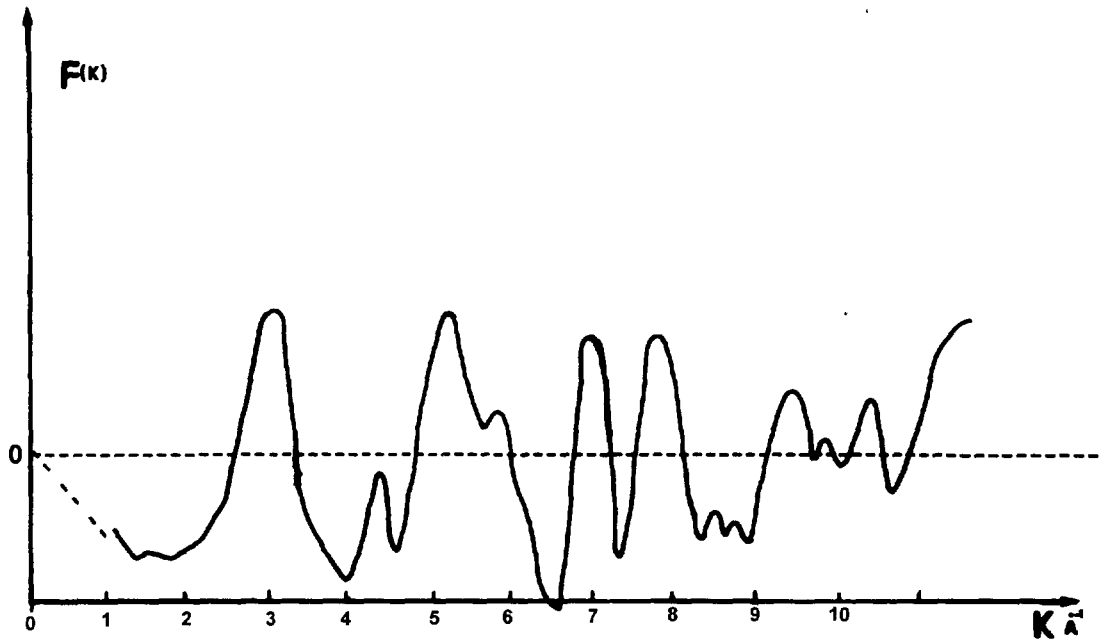


Fig. 7. — The reduced interference function $F(K)$ derived from $I_d(\theta)$. For the first peak $K_1 = 2.95 \text{ \AA}^{-1}$, second: $K_2 = 4.90 \text{ \AA}^{-1}$, 3th: $K_3 = 4.90 \text{ \AA}^{-1}$, and $K_2/K_1 = 1.66 \rightarrow$ the signature of the random dense packing model. The local order in this structure has an *icosahedral symmetry*.

reported that in the structure of Frank-Kasper the anomalous coordinations (*i.e.* [14–16]) form infinite FK chains and the chains themselves form ordered arrays [23].

Recent views on structures of metallic amorphous alloys, propose similar concepts where theoretical and experimental studies have been taken to account. It can also be added that polytetrahedral glasses can be regarded as FK structures in which the anomalous chains are disordered [21].

In order to describe the amorphous structure, the curved space concepts were used (for a general review on this topic, see Venkateraman, Sahoo and references therein [22]). In this space a perfect tetrahedral can be defined as a $\{3, 3, 5\}$ polytope. This polytope and the complementary $\{5, 3, 3\}$ polytope, have been the focus of structural studies of the Frank-Kasper phase, such as the A_2B (Laves phases) and the A_5B (Hauck phases). The model which is used for describing these structures is a hierarchical model. In this model the rotational defect lines *i.e.* the disclination lines are generated by a simple iterative succession of decurving processes. These gradually decrease the curvature of a $\{5, 3, 3\}$ polytope model and then render a geometrical model in normal space for non-crystalline material.

The occurrence of disclination networks or the FK chains in the Frank and Kasper crystalline and amorphous phases can be justified by comparing the partial interference functions, the inter atomic distances and the coordination numbers (see Ref. [21]). These quantitative results, have been achieved for the first time (*cf.* references obtained from the structural studies of the amorphous FK phase [21]).

An imaginary qualitative scenario has been suggested, for transforming liquids, during a cool-down with different cooling rates, into either the FK crystal or the FK amorphous or

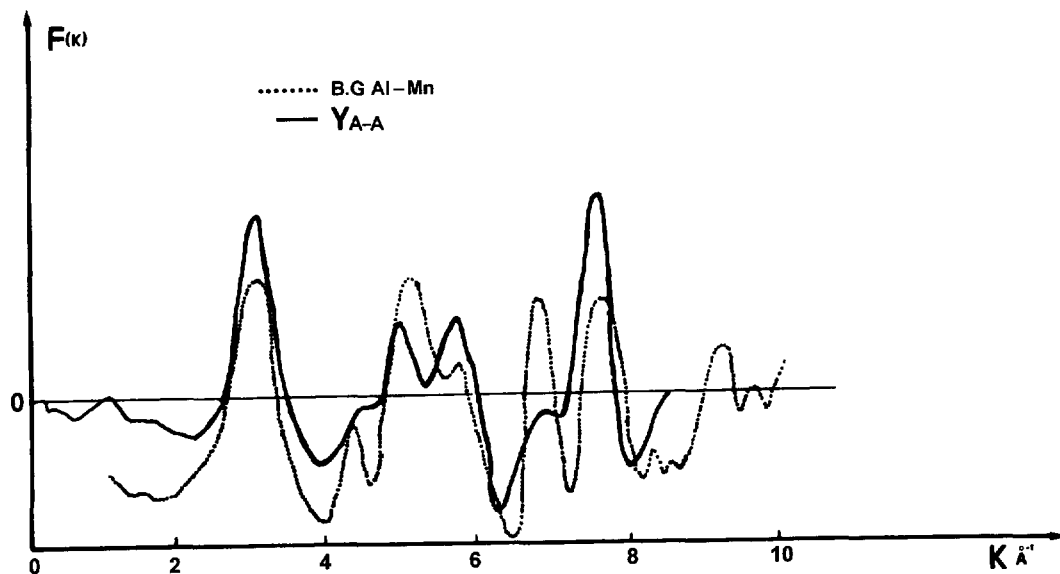


Fig. 8. — This figure shows a strong correlation between the maximum position of the experimental $F(K)$ of BG and the theoretical geometrical model (Ref. [21]) Even the small humps fitted.

other unusual structures such as polymer like chains. Sharp lines superimposed on rings in the X-ray diagram of any polymer confirm the viability of “the imaginary” structural proposition. Recently, in numerous structural studies of polyaniline (Polymers [24]) similar short range orders in crystalline and amorphous states have been reported.

The behaviour of total interference functions of the rings (Fig. 8) are crudely comparable to the partial interference functions of the disordered FK phases. Despite the strong correlation in the peak positions of these two functions it should be mentioned that it is only through the knowledge of experimental partial functions that these comparisons would be credible. This type of analogy assumes that *the FK chain (line defects) is a part of the substance which is responsible for the scattered rings.*

3.2.2. Radial Distribution Functions (R.D.F.). — Another approach for acquiring structural information from the part which is responsible for rings is the determination of the reduced radial distribution function $W(r)$.

This function is derived from the Fourier Transformation of the reduced interference function ($F(k)$) which represents the average contribution of all the distinct atomic pairs in the structure of these parts. In the interval: $0 < K < 18 \text{ \AA}^{-1}$ the experimental $F(k)$ curve is analytically normalized: according to the above arguments there are no inter atomic distances smaller than the nearest - neighbour distance. This indicates that the curve below the first peak of the RDF has a slope of “-1”.

Figure 9 shows that we have succeeded in obtaining such a slope. This achievement has resulted from the careful separation of the elastic and inelastic components of the scattered X-ray beam and the useful separation of the line spectra from the ring diagrams. From these, a high quality $F(k)$ was obtained. Table II indicates the positions of the first maxima (in \AA). The r max. of $W(r)$ of the background is shown in Figure 9.

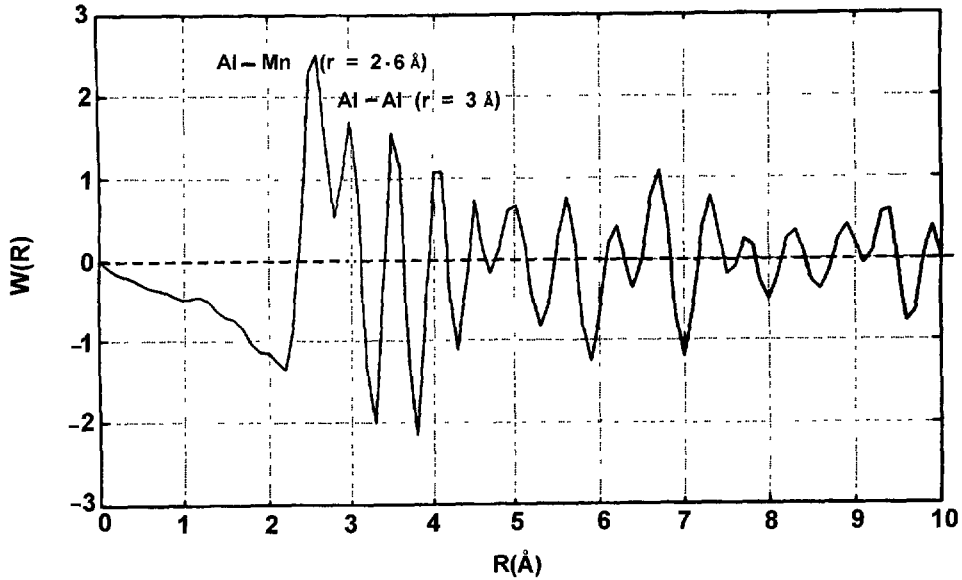


Fig. 9. — The reduced radial distribution function derived by Fourier transform from $F(K)$.

Table II. — Interatomic distances between the different atoms of metastable Al_6Mn phase. (r_n : the position in real space of the n^{th} oscillations).

r_n	r_1	r_2	r_3	r_4	r_5	r_6	r_7
Å	2.6	3	3.4	3	4.4	5	7.3

These (r_n) values are attributed to the inter atomic distances between the different atoms of this metastable alloy compound: (Al-Mn). The Goldschmidt radius of Al is close to 1.43 Å and Mn = 1.35 Å. The first r_1 can be attributed to Al-Mn ($r_{Al} + r_{Mn} = 2.78$ Å or Mn ($r_{Mn} + r_{Mn} = 2.71$ Å). However, in two cases the value obtained by this experiment is smaller than these values.

For structural investigations, numerous workers [25, 26] have been interested in using the structural determination of the crystalline intermetallic compound (Al_6Mn) of this metastable phase. In these studies they have reported that "the powder pattern of Al_6Mn is too complex to interpret without ambiguity" [25]. The structural determination was performed by using single crystals.

The average nearest neighbour to the Mn-Al distance has been reported to be 2.56 ± 0.04 and the Al-Al = $2.78 \text{ Å} \pm 0.04$. Therefore $r_1 = 2.60$ Å obtained from the $W(r)$ of background can be logically attributed to the Mn-Al of the first neighbouring distance and not the Mn-Mn distance. The integration of this peak gives a coordination number of $N_c = 8.96$ (with $d = 3.5 \text{ g/cm}^3$ see Ref. [27]) which is between N_c (Mn-Al) = 10 and N_c (Al-Mn) = 7. $r_2 = 2.95$ Å can be attributed to Al-Al which is rather larger than $Al_2-Al_3 = 2.89 \pm 0.045$ Å obtained in crystalline order. Obviously a discrepancy rises from the values which are obtained from the total $W(r)$ that gives the average distances of different Al-Al sites.

In Al_6Mn three sites have been reported for Al which vary from $\text{Al}_2\text{-Al}_2 = 2.56 \text{ \AA}$ up to $\text{Al}_3\text{-Al}_2 = 2.89 \text{ \AA}$. Certainly, for obtaining more precise structural information about the "environment" of each component anomalous diffraction techniques have to be used. Currently using this technique, we are obtaining partial atomic distribution functions of specific atomic species. Despite this, we should conclude that the first neighbour distance of Mn-Mn does not exhibit the properties reported for its crystal counterpart phase (Al_6Mn).

3.3. CONCLUDING REMARKS. — The X-ray patterns of splat cooled Al-Mn characterized by sharp lines superimposed on rings have been obtained. Unlike the traditional way used for indexing powder patterns, the method of "separation" of the lines from the rings, for interpreting this X-ray diagram, has been introduced in this work. For the first time, using these rings (a coherent background) the correlation positions were deduced from a high quality interference function. These results indicate the structural relationship between the intermetallic complex phases and this phase. A total RDF of the background indicates that the Mn-Mn contacts are avoided in the first neighbour as a Frank unit in the supercooled liquid.

This following approach may be used for comprehending the structural relationships.

When the cooling rates changed during solidification, these units are converted into infinite FK chains (skeleton), which are of three types: ordered chains (polytetrahedral crystals), disordered chains (amorphous polytetrahedral) and quasi-ordered chains (in Al_6Mn); which then result in the propagation of the icosahedral order.

The network of the lines' defect (FK chain) diffracts a different X-ray pattern *i.e.* the rings, the rings have a pre-peak, the lines are superimposed on the rings and the sharp lines (the delta function). This is an indication of the different *degrees of disorder*.

In order to understand this approach we still need more structural information, such as the interatomic distances and the coordination numbers of this alloy. This information can be found in the partial pair-pair correlation function of the background. By using a convenient geometrical model the organization of the disordered FK chains can be achieved by layer structures which also diffract the Bragg reflection.

References

- [1] Levine D. and Steinhardt P.J., *Phys. Rev. Lett.* **53** (1984) 2477.
- [2] Shechtman D.S., Blech I., Gratias D. and Cahn J.W., *Phys. Rev. Lett.* **53** (1984) 1951.
- [3] Pauling L., *Nature London* **317** (1985) 512.
- [4] Pauling L., *Phys. Rev. Lett.* **58** (1987) 365.
- [5] Anantharaman T.R., *Current Sci.* **57** (1988) 578-586.
- [6] Ramachandrarao P., Laridjani M. and Cahn R.W., *Z. Metallik* **63** (1972) 43.
- [7] Laridjani M., Krishnan K.D. and Cahn R.W., *J. Mater. Sci.* **11** (1976) 1643-1652.
- [8] Mozer B., Cahn J.W. and Gratias D., *J. Phys. Colloq. France* **47** (1986) C3-351.
- [9] Bancel P.A. and Heiney P.A., *J. Phys. Colloq. France* **47** (1986) C3-341.
- [10] Laridjani M. and Sadoc J.F., *J. Phys. France* **48** (1987) 114.
- [11] Laridjani M., Leboucher P. and Sadoc J.F., *Spectre 2000* **16** (1988) 25.
- [12] Laridjani M., Sadoc J.F. and Raoux D., *J. Non-Cryst. Solids* **91** (1987) 217-234.
- [13] Sandstrom A.E., in "Handbuch der Physik", S. Flügge Ed. (Springer, Berlin, 1957) pp. 217-234.

- [14] Bancel P.A., Heiney P.A., Stephen P.W., Goldman A.F. and Horn P.M., *Phys. Rev. Lett.* **54** (1985) 2422.
- [15] Shechtman D. and Blech I.A., *Met. Trans. A* **16A** (1985) 1005.
- [16] Shechtman D., Blech F.A., Gratias D. and Cahn J.W., *Phys. Rev. Lett.* **53** (1984) 1951.
- [17] Sadoc J.F., Dixmier J. and Guimer A., *J. Non-Cryst-Solids* **12** (1973) 46-60.
- [18] Hume-Rothery W. and Anderson E., *Proc. Roy. Soc. A* **383** (1959).
- [19] Laridjani M., Luzet D. and Perrin M., unpublished paper, the work has been done at CEN Saclay France (1980).
- [20] Frank F.C., *Proc. Roy. Soc. A* **215** (1952) 43.
- [21] Laridjani M. and Sadoc J.F., *J. Phys. France* **50** (1989) 1953-1966.
- [22] Venkatarman G. and Sahoo D., *Contemp. Phys.* **26** (1985) 579-615.
- [23] Frank F.C. and Kasper J.S., *Acta Cryst.* **12** (1959) 483.
- [24] Laridjani M., Pouget J.P., Scherr E.M., MacDiarmid A.G., Jozefowicz M.E. and Epstein A.J., *Macromolecules* **25** (1992).
- [25] Raynor G.V. and Hume-Rothery W., *Proc. Roy. Soc. A* **205** (1951) 103.
- [26] Nicol A.D.I., *Acta Cryst.* **6** (1953) 285.
- [27] Kelton K.F. and Wu T.W., *Appl. Phys. Lett.* **46** (1985) 1059.